Supporting Information

Identification of Metabolites in Basil Leaves by Desorption Electrospray Ionization Mass Spectrometry Imaging after Cd Contamination

Vânia de Lourdes G. Teles[1,2], Giselle V. Sousa[1], Pedro H. Vendramini[3], Rodinei Augusti[4] and Letícia M. Costa*[1]

[1]*LEAQUAA, Universidade Federal de Minas Gerais, Instituto de Ciências Exatas, Departamento de Química, CEP 31270-901, Belo Horizonte, Minas Gerais, Brazil.*

[2]*Universidade Estadual de Roraima, CEP 69306-530, Boa Vista, Roraima, Brazil*

[3] *ThoMSon Mass Spectrometry Laboratory, IQ-UNICAMP, CEP 13083-970, Campinas, São Paulo, Brazil.*

[4]*LEMS, Universidade Federal de Minas Gerais, Instituto de Ciências Exatas, Departamento de Química, CEP 31270-901, Belo Horizonte, Minas Gerais, Brazil.*

* Email: leticia@qui.ufmg.br, lemalta41@gmail.com; Phone: +55 31 3409 5764

List of Supporting Information

Table S1. CCD results for the optimization of Cd concentration in basil leaves (L), stems (S) and roots (R)

Table S2. LOD and LOQ of the ultrasound-assisted micro-extraction procedure for Cd determination by FS FAAS

Figure S1. Cd concentration in acid solutions containing micronutrients, macronutrients and multi-element solutions: low (0.1 mg L^{-1} Cu, Fe, Mn and Zn and 200 mg L^{-1} Ca, K and Mg), middle (0.15 mg L^{-1} Cu, Fe, Mn and Zn and 400 mg L^{-1} Ca, K and Mg) and high (0.2 mg L^{-1} Cu, Fe, Mn and Zn and 600 mg L^{-1} Ca, K and Mg) (n = 3).

Figure S2. Pictures of leaves of basil, control (without Cd^{2+}) and 10 µmol L^{-1} Cd^{2+} exposure, in double-sided adhesive tape to direct analysis by DESI-MSI

Figure S3. DESI images of phytohormones in leaves of basil, control (without Cd^{2+}) and 10 µmol L^{-1} Cd^{2+} exposure: (a) jasmonic acid (Na^+ adduct, *m/z* 233.11147), (b) methyl dihydrojasmonate (Na^+ adduct, *m/z* 249.1460), (c) abscisic acid (Na^+ adduct, *m/z* 287.1252), (d) (-)-jasmonoyl-L-isoleucine (*m/z* 324.2167), (e) auxin b (Na^+ adduct, *m/z* 333.2037) and (f) auxin a (Na^+ adduct, *m/z* 351.2138). The pixel size is 200 µm.

Figure S4. DESI image of sugars in leaves of basil, control (without Cd^{2+}) and 10 µmol L^{-1} Cd^{2+} exposure: (a) carbohydrates (Na^+ adduct, *m/z* 335.0947) and (b) disaccharide (Na^+ adduct, *m/z* 365.1053). The pixel size is 200 µm.

Figure S5. DESI image of amino acids in leaves of basil, control (without Cd^{2+}) and 10 µmol L-1 Cd^{2+} exposure: (a) amino acids (*m/z* 118.0864) (b) leucine (*m/z* 132.1019), (c) glutamine (*m/z* 147.0764), (d) arginine (*m/z* 175.1191), (e) peptides (($[M+H-2H_2O]^+$, *m/z* 293.0598), (f) peptides (*m/z* 306.1601), (g) peptides (*m/z* 435.2355), (h) peptides ((*m/z* 613.2468). The pixel size is 200 µm.

Figure S6. DESI image of other metabolites in leaves of basil, control (without Cd^{2+}) and 10 µmol L^{-1} Cd^{2+} exposure: (a) choline (*m/z* 104.1073), (b) spermidine (*m/z* 146.1652), (c) fatty acid esters (Na^+ adduct, *m/z* 169.0471), (d) jasmolone glucoside (Na^+ adduct, *m/z* 365.1571) and (e) methylpicraquassioside A (K^+ aduct, *m/z* 451.1004). The pixel size is 200 µm.

Figure S7. Expanded view (from *m/z* 100 to 300) of the average MS (positive ion mode) of amino acids obtained (a) line 25 of the control leaf of basil (without Cd^{2+}) and (b) line 81 of the contaminated basil leaf (10 µmol L^{-1} Cd^{2+}). Amplifications, indicated above each ion, were used to facilitate visualization in Mass Spectrum. The *m/z* ratios are indicated above each amino acid.

Figure S8. Expanded view (from *m/z* 300 to 650) of the average MS (positive ion mode) of amino acids obtained (a) line 25 of the control leaf of basil (without Cd^{2+}) and (b) line 81 of the contaminated basil leaf (10 µmol L^{-1} Cd^{2+}). Amplifications, indicated above each ion, were used to facilitate visualization in Mass Spectrum. The *m/z* ratios are indicated above each amino acid.

Figure S9. Expanded view (from *m/z* 295 to 500) of the average MS (positive ion mode) of flavonoids obtained line 78 of the contaminated leaf of basil (10 µmol L^{-1} Cd^{2+}). Amplifications, indicated above each ion, were used to facilitate visualization in Mass Spectrum. The *m/z* ratios are indicated above each flavonoid.

Figure S10. Expanded view (from *m/z* 150 to 400) of the average MS (positive ion mode) of phytohormones obtained (a) line 25 of the control leaf of basil (without Cd^{2+}) and (b) line 80 of the contaminated leaf of basil (10 µmol L^{-1} Cd^{2+}). Amplifications, indicated above each ion, were used to facilitate visualization in Mass Spectrum. The *m/z* ratios are indicated above each phytohormone.

Figure S11. Expanded view (from *m/z* 200 to 400) of the average MS (positive ion mode) of sugars obtained (a) line 7 of the control leaf of basil (without Cd^{2+}) and (b) line 78 of the contaminated leaf of basil (10 µmol L^{-1} Cd^{2+}). Amplifications, indicated above each ion, were used to facilitate visualization in Mass Spectrum. The *m/z* ratios are indicated above each sugar

Figure S12. Expanded view (from *m/z* 100 to 500) of the average MS (positive ion mode) of common compounds in plants obtained (a) line 25 of the control leaf of basil (without Cd^{2+}) and (b) line 80 of the contaminated leaf of basil (10 µmol L^{-1} Cd^{2+}). Amplifications, indicated above each ion, were used to facilitate visualization in Mass Spectrum. The *m/z* ratios are indicated above each compound.

Table S1. CCD results for the optimization of Cd concentration in basil leaves (L), stems (S) and roots (R)

Experiment	HNO_3 (%)	H_2O_2 (µL)	Concentration in Matrix (µg g^{-1})			OR (µg g^{-1})
			L	S	R	
1	2	50	106	277	1193	2.38
2	2	100	137	332	1199	2.76
3	10	50	102	309	1201	2.44
4	10	100	96.5	290	1161	2.32
5	12	75	122	322	1175	2.60
6	0.4	75	107	340	1421	2.72
7	6	110	104	285	1440	2.55
8	6	40	73.4	243	1072	1.96
CP	6	75	88.5	290	1346	2.39
CP	6	75	99.1	320	1371	2.57
CP	6	75	92.2	279	1317	2.37
CP	6	75	86.5	358	1356	2.57

$$OR_{Cd} = 2.47 - 0.0674x_A + 0.1377x_B - 0.1259x_{AB} + 0.0959x_A^2 - 0.1055\, x_B^2$$

where, 2.47 is the average from the total observations whereas $x_{A,}$ x_B and x_{AB} represent the effects of each factor, i.e. A, B and their interaction, respectively. The average for predicted values was approximately 2.5, confirming that the response surface model for two factors was accurate, according to the equation. CP = central point

Table S2 LOD and LOQ of the ultrasound-assisted micro-extraction procedure for Cd determination by FS FAAS

Regression Equation	Correlation coefficient (R)	Method		Matrix	Sample	
		LOD (µg L^{-1})	LOQ (µg L^{-1})		LOD (µg kg^{-1})	LOQ (µg kg^{-1})
y = 0.216x + 0.004	0.991	6	17	L	61	111
				S	66	100
				R	104	139

For the method, LOD and LOQ = 3 and 10 times the standard deviation of the blank solution, divided by the slope of the calibration curve, respectively. For the blank samples, LOD and LOQ were $\overline{X} + t(n\text{-}1,\, 1\text{-}\alpha).s$ and $\overline{X} + 10.\,s$, respectivel, where $\overline{X}$ is the average of the blank samples values, s is the standard deviation and t-distribution at 95% confidence level.

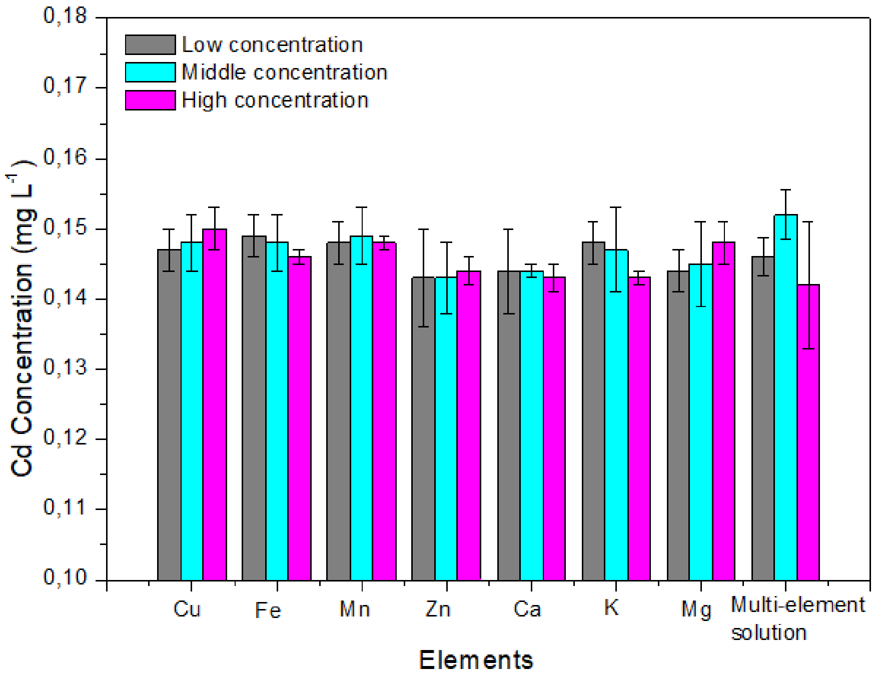

Figure S1. Cd concentration in acid solutions containing micronutrients, macronutrients and multi-element solutions: low (0.1 mg L^{-1} Cu, Fe, Mn and Zn and 200 mg L^{-1} Ca, K and Mg), middle (0.15 mg L^{-1} Cu, Fe, Mn and Zn and 400 mg L^{-1} Ca, K and Mg) and high (0.2 mg L^{-1} Cu, Fe, Mn and Zn and 600 mg L^{-1} Ca, K and Mg) (n = 3).

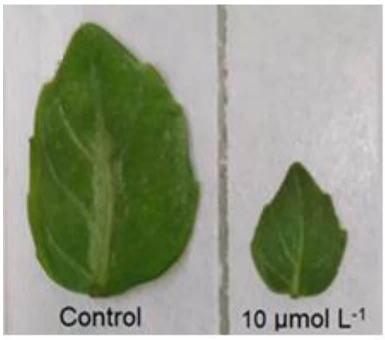

Figure S2. Pictures of leaves of basil, control (without Cd^{2+}) and 10 µmol L^{-1} Cd^{2+} exposure, in double-sided adhesive tape to direct analysis by DESI-MSI

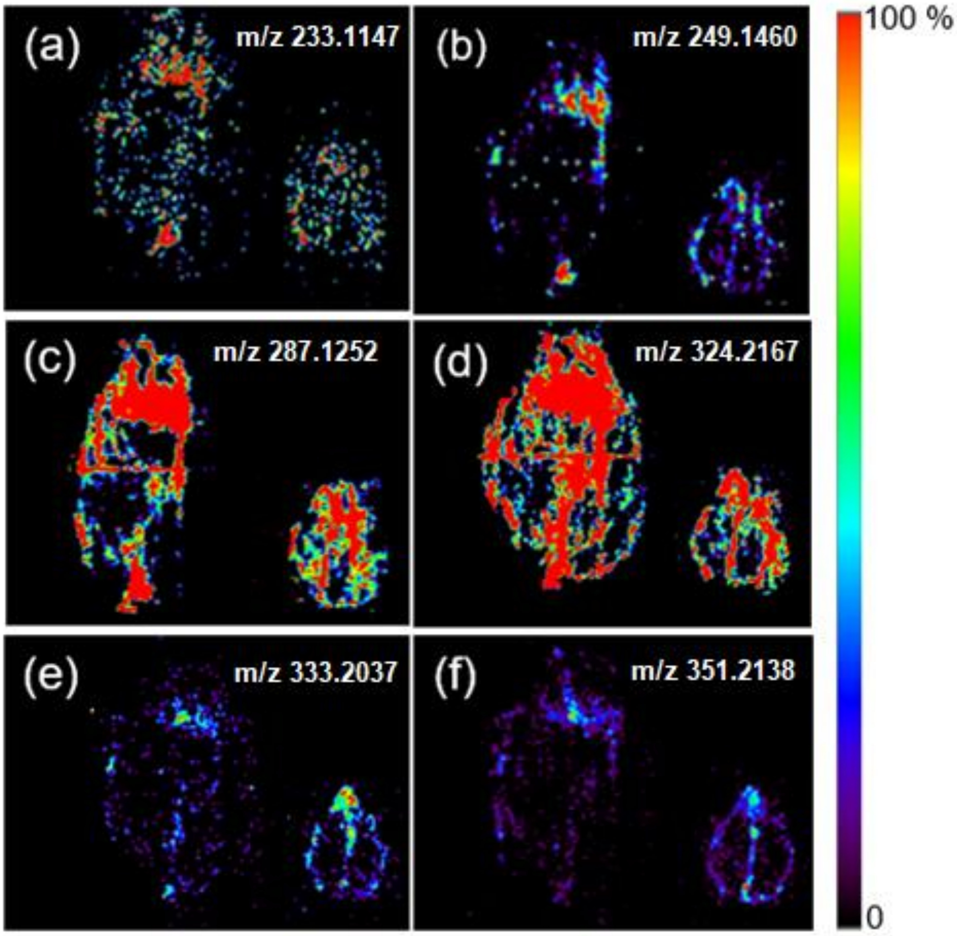

Figure S3. DESI images of phytohormones in leaves of basil, control (without Cd^{2+}) and 10 µmol L^{-1} Cd^{2+} exposure: (a) jasmonic acid (Na^{+} adduct, *m/z* 233.11147), (b) methyl dihydrojasmonate (Na^{+} adduct, *m/z* 249.1460), (c) abscisic acid (Na^{+} adduct, *m/z* 287.1252), (d) (-)-jasmonoyl-L-isoleucine (*m/z* 324.2167), (e) auxin b (Na^{+} adduct, *m/z* 333.2037) and (f) auxin a (Na^{+} adduct, *m/z* 351.2138). The pixel size is 200 µm.

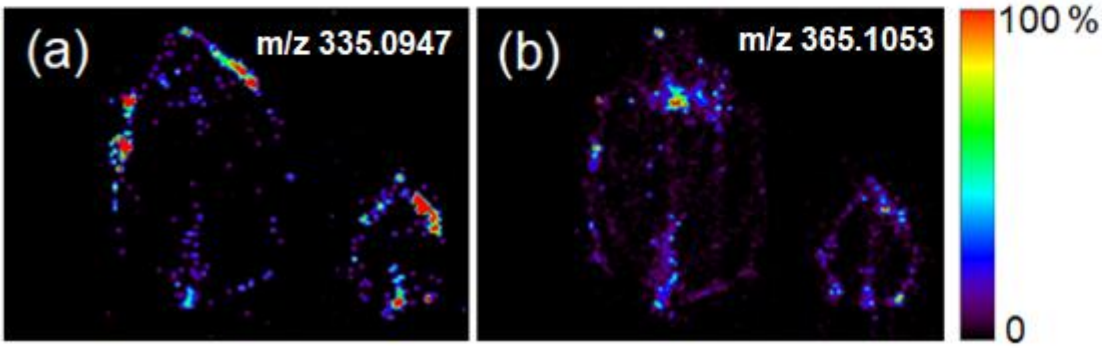

Figure S4. DESI image of sugars in leaves of basil, control (without Cd^{2+}) and 10 µmol L^{-1} Cd^{2+} exposure: (a) carbohydrates (Na^+ adduct, *m/z* 335.0947) and (b) disaccharide (Na^+ adduct, *m/z* 365.1053). The pixel size is 200 µm.

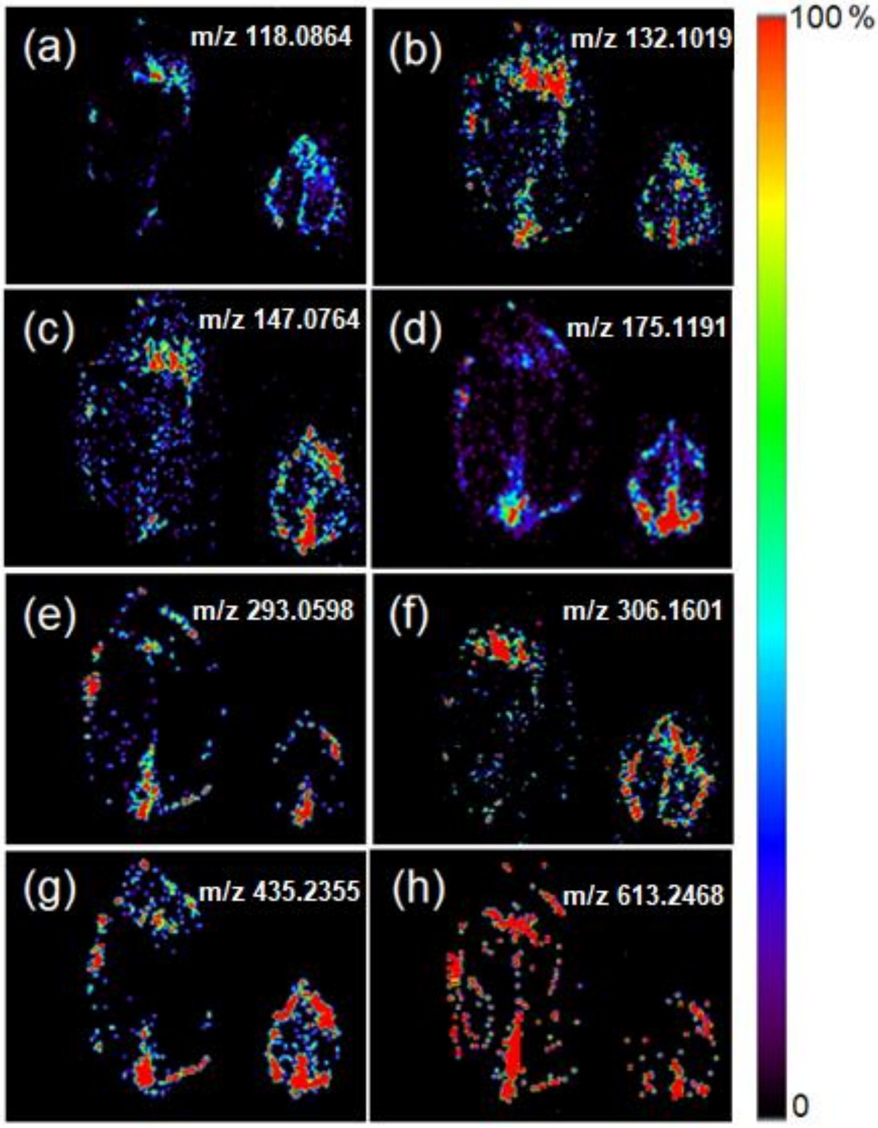

Figure S5. DESI image of amino acids in leaves of basil, control (without Cd^{2+}) and 10 µmol L-1 Cd^{2+} exposure: (a) amino acids (*m/z* 118.0864) (b) leucine (*m/z*

132.1019), (c) glutamine (*m/z* 147.0764), (d) arginine (*m/z* 175.1191), (e) peptides (([M+H-2H_2O]$^+$, *m/z* 293.0598), (f) peptides (*m/z* 306.1601), (g) peptides (*m/z* 435.2355), (h) peptides ((*m/z* 613.2468). The pixel size is 200 μm.

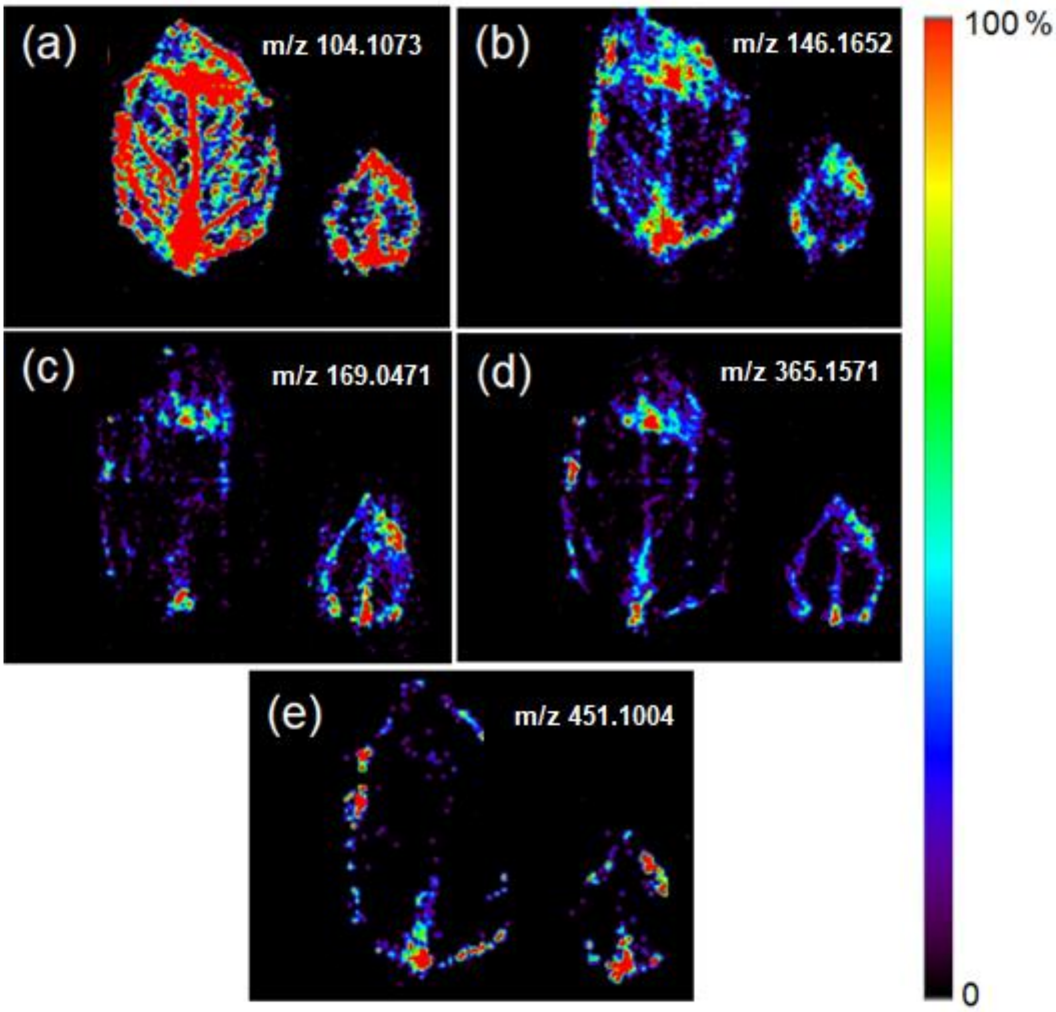

Figure S6. DESI image of other metabolites in leaves of basil, control (without Cd^{2+}) and 10 μmol L^{-1} Cd^{2+} exposure: (a) choline (*m/z* 104.1073), (b) spermidine (*m/z* 146.1652), (c) fatty acid esters (Na^+ adduct, *m/z* 169.0471), (d) jasmolone glucoside (Na^+ adduct, *m/z* 365.1571) and (e) methylpicraquassioside A (K^+ aduct, *m/z* 451.1004). The pixel size is 200 μm.

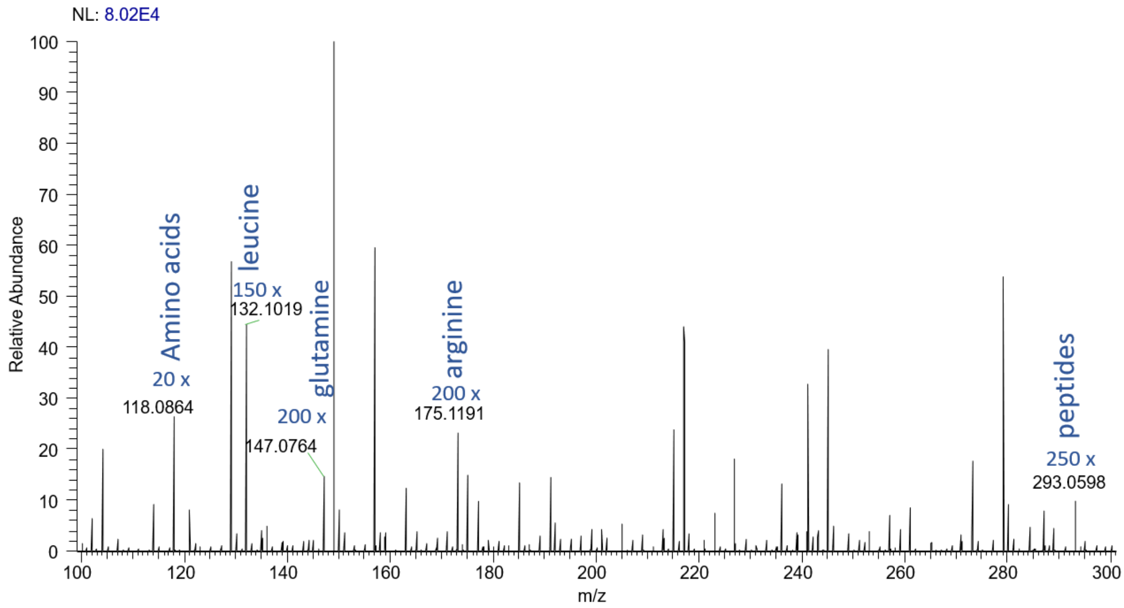

(a) Control leaf

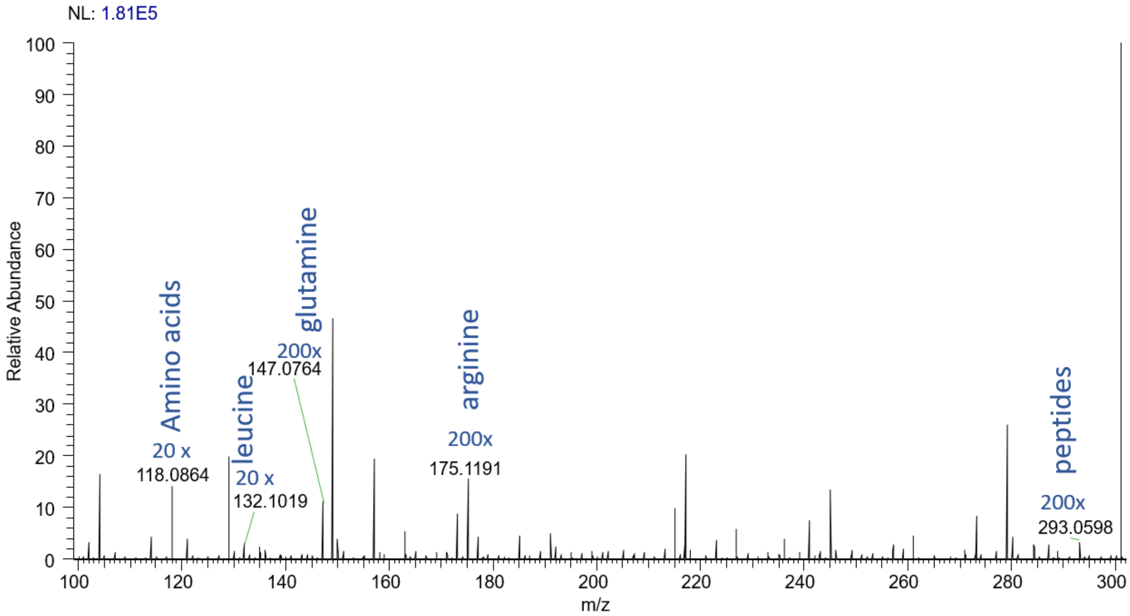

(b) Leaf exposure to Cd^{2+} (10 µmol L^{-1} Cd^{2+})

Figure S7. Expanded view (from *m/z* 100 to 300) of the average MS (positive ion mode) of amino acids obtained (a) line 25 of the control leaf of basil (without Cd^{2+}) and (b) line 81 of the contaminated leaf of basil (10 µmol L^{-1} Cd^{2+}). Amplifications, indicated above each ion, were used to facilitate visualization in Mass Spectrum. The *m/z* ratios are indicated above each amino acid.

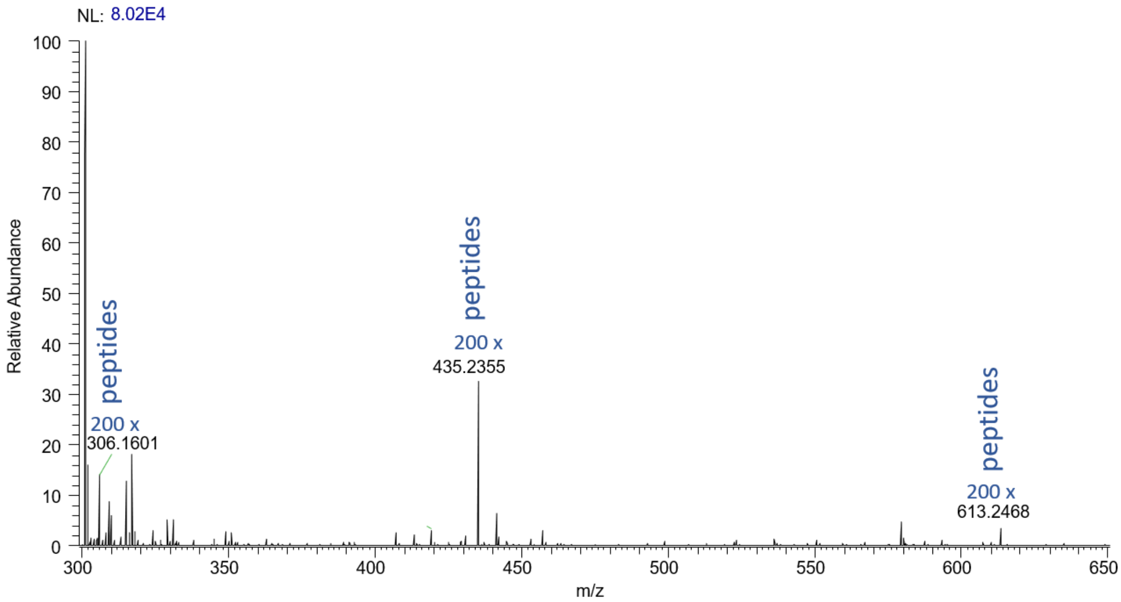

(a) Control leaf

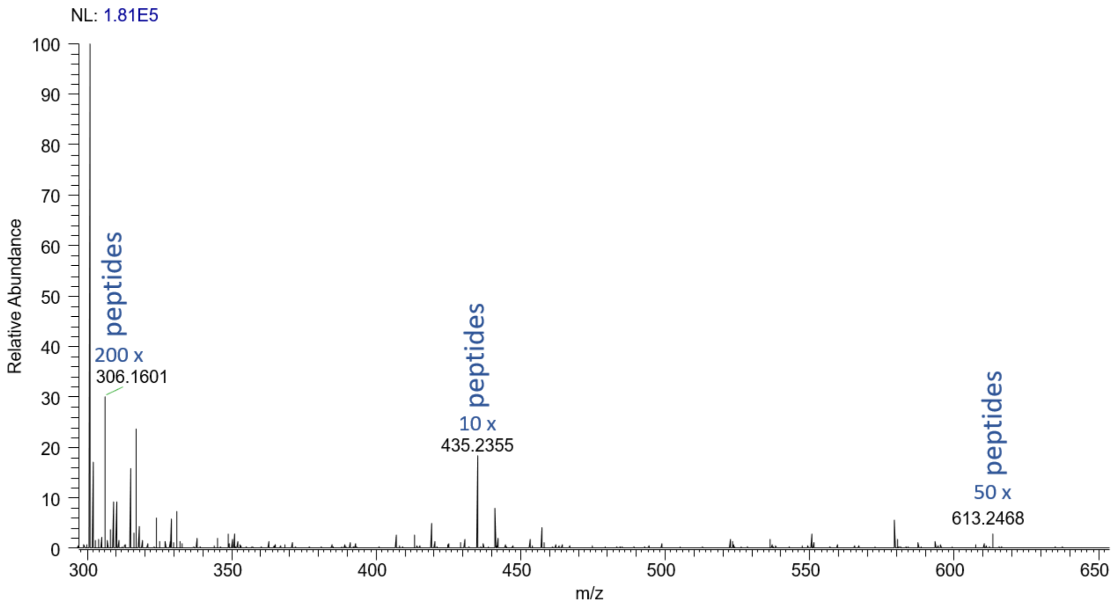

(b) Leaf exposure to Cd^{2+} (10 µmol L^{-1} Cd^{2+})

Figure S8. Expanded view (from *m/z* 300 to 650) of the average MS (positive ion mode) of amino acids obtained (a) line 25 of the control leaf of basil (without Cd^{2+}) and (b) line 81 of the contaminated leaf of basil (10 µmol L^{-1} Cd^{2+}). Amplifications, indicated above each ion, were used to facilitate visualization in Mass Spectrum. The *m/z* ratios are indicated above each amino acid.

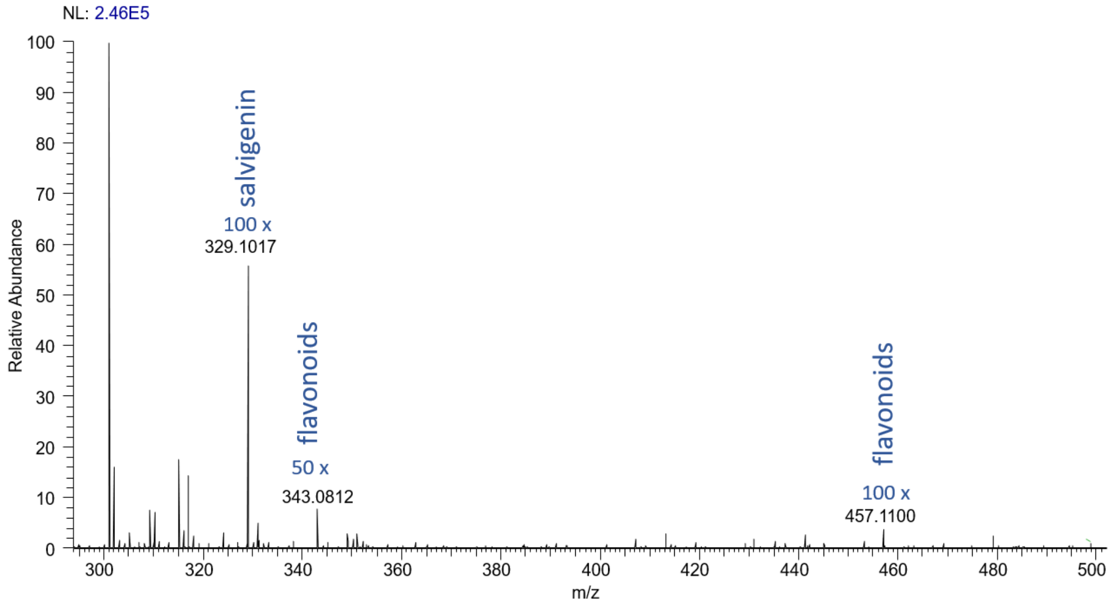

Figure S9. Expanded view (from *m/z* 295 to 500) of the average MS (positive ion mode) of flavonoids obtained line 78 of the contaminated leaf of basil (10 µmol L^{-1} Cd^{2+}). Amplifications, indicated above each ion, were used to facilitate visualization in Mass Spectrum. The *m/z* ratios are indicated above each flavonoid.

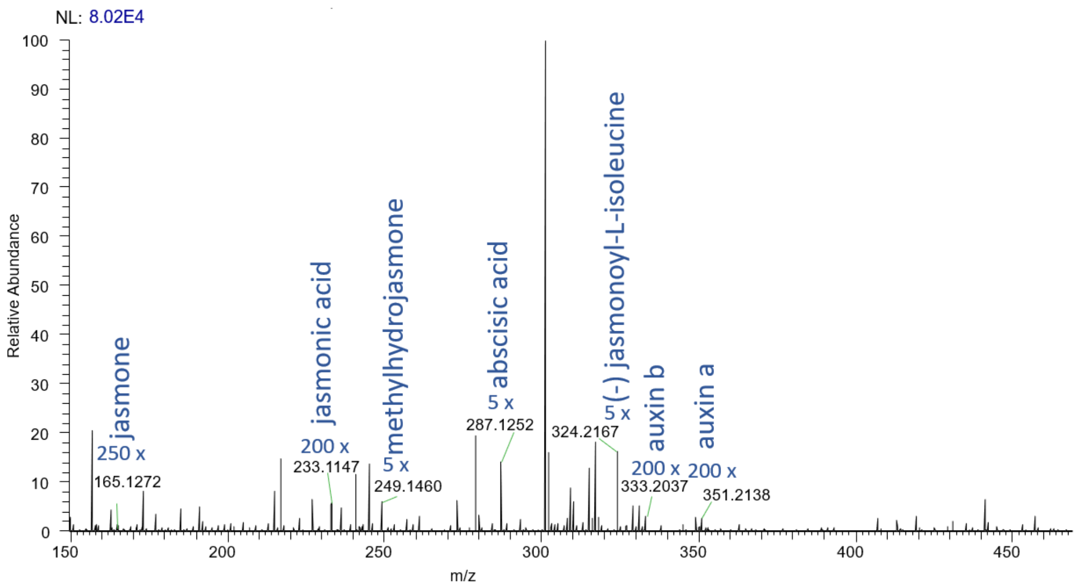

(a) Control leaf

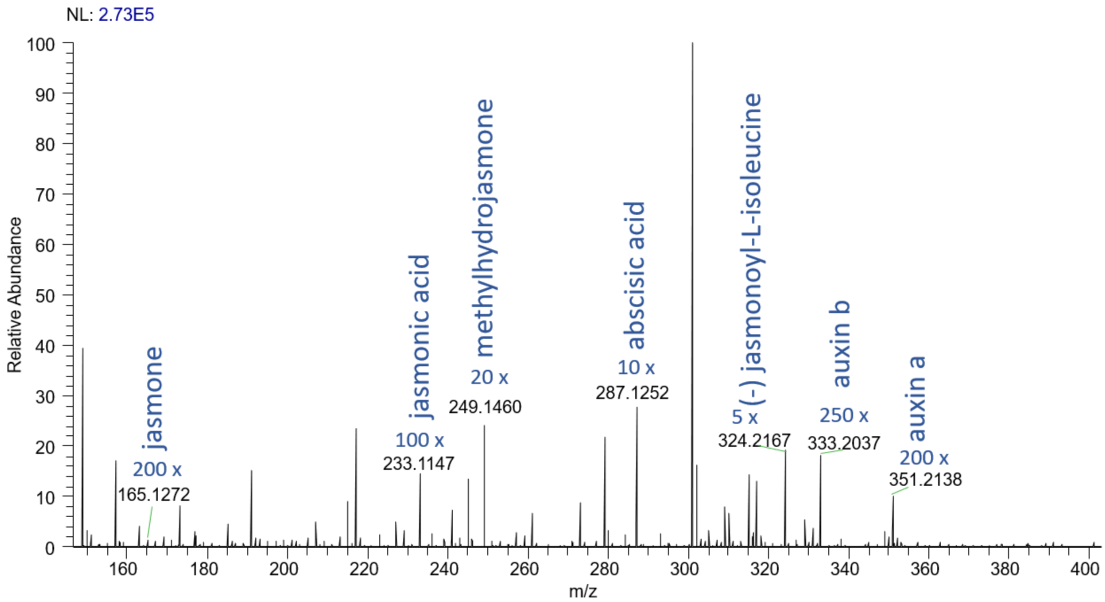

(b) Leaf exposure to Cd^{2+} (10 µmol L^{-1} Cd^{2+})

Figure S10. Expanded view (from *m/z* 150 to 400) of the average MS (positive ion mode) of phytohormones obtained (a) line 25 of the control leaf of basil (without Cd^{2+}) and (b) line 80 of the contaminated leaf of basil (10 µmol L^{-1} Cd^{2+}). Amplifications, indicated above each ion, were used to facilitate visualization in Mass Spectrum. The *m/z* ratios are indicated above each phytohormone.

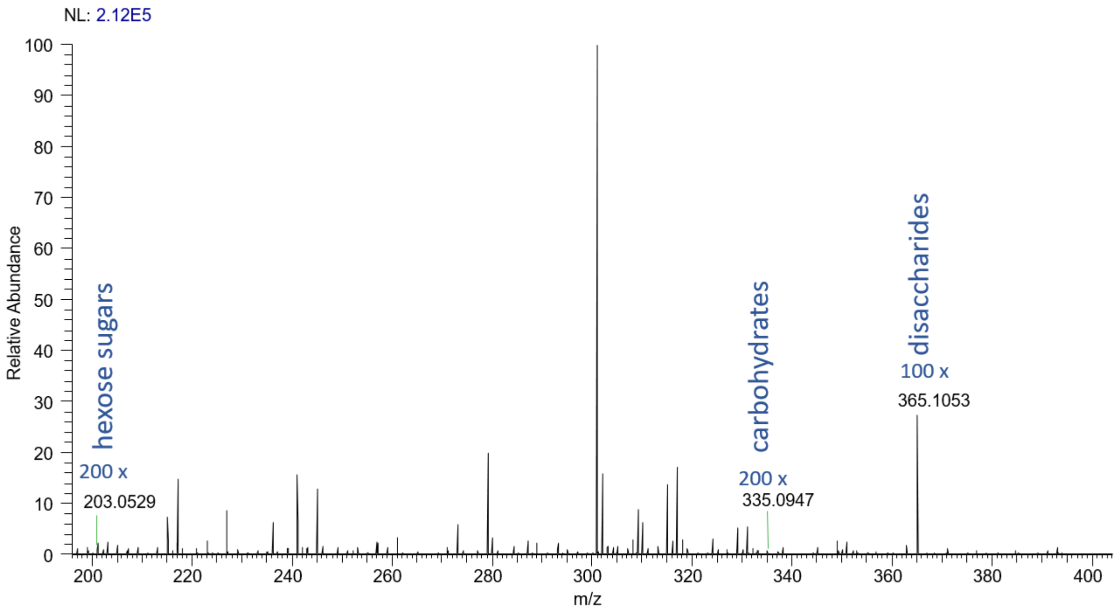

(a) Control leaf

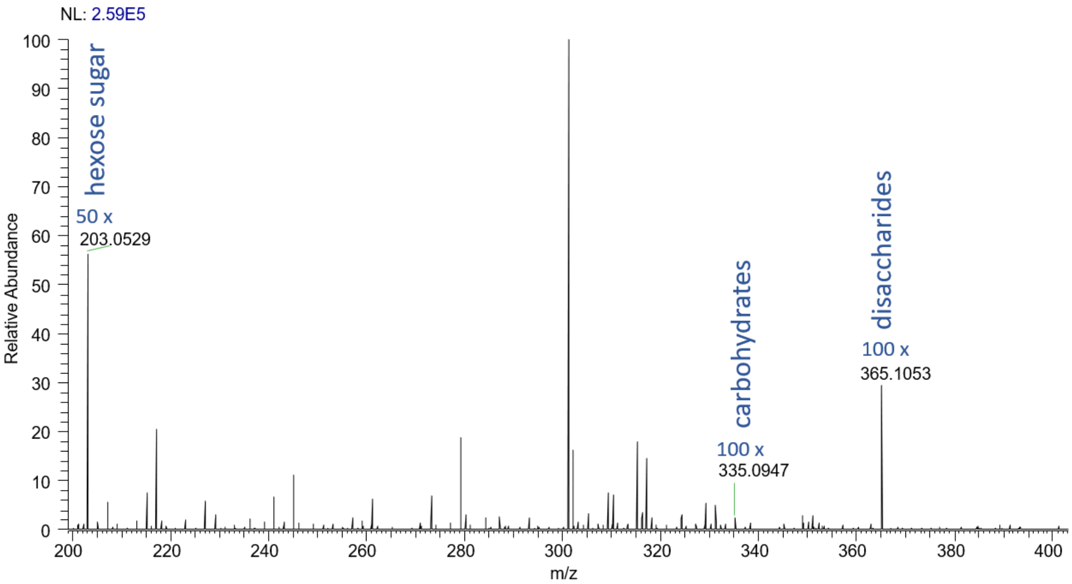

(b) Leaf exposure to Cd^{2+} (10 µmol L^{-1} Cd^{2+})

Figure S11. Expanded view (from *m/z* 200 to 400) of the average MS (positive ion mode) of sugars obtained (a) line 7 of the control leaf of basil (without Cd^{2+}) and (b) line 78 of the contaminated leaf of basil (10 µmol L^{-1} Cd^{2+}). Amplifications, indicated above each ion, were used to facilitate visualization in Mass Spectrum. The *m/z* ratios are indicated above each sugar

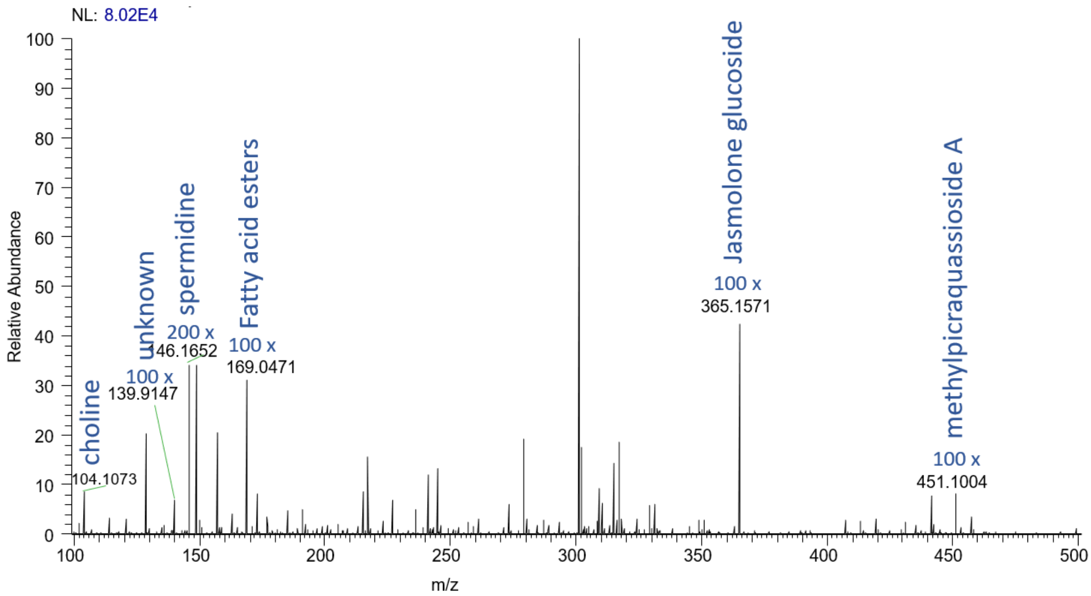

(a) Control leaf

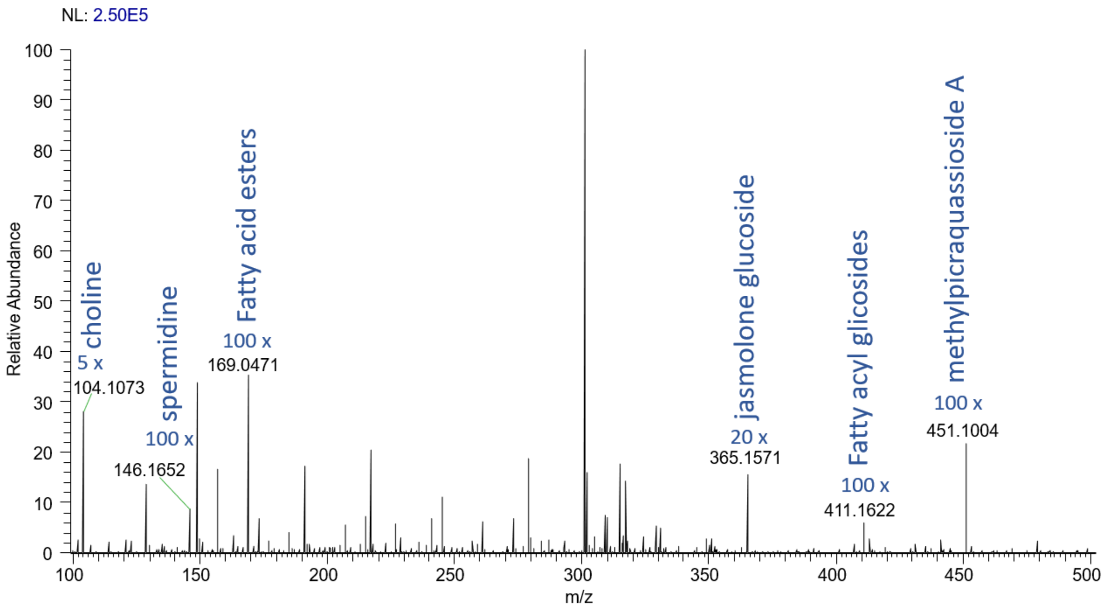

(b) Leaf exposure to Cd^{2+} (10 µmol L^{-1} Cd^{2+})

Figure S12. Expanded view (from *m/z* 100 to 500) of the average MS (positive ion mode) of common compounds in plants obtained (a) line 25 of the control leaf of basil (without Cd^{2+}) and (b) line 80 of the contaminated leaf of basil (10 µmol L^{-1} Cd^{2+}). Amplifications, indicated above each ion, were used to facilitate visualization in Mass Spectrum. The *m/z* ratios are indicated above each compound.